

Effects of host heterogeneity on parasite transmission are mediated by the dynamics of infectiousness determination.

Jacob A. Cohen¹ (jacob.cohen@liverpool.ac.uk), Andrew D. Dean¹ (andrew.dean@liverpool.ac.uk), Mark Viney¹ (mev@liverpool.ac.uk), Andy Fenton¹ (acf1@liverpool.ac.uk)

1. Department of Evolution, Ecology and Behaviour, Institute of Infection, Veterinary and Ecological Sciences, University of Liverpool, Liverpool L69 7ZB, UK.

Author contributions: JAC, AF and MV jointly conceived the research. JAC conducted the research and formal analysis. ADD contributed considerably to the formal analysis. JAC wrote the first draft of the manuscript, and all authors contributed substantially to revisions.

Data accessibility statement: The data and code that support the findings of this study are available through [http://data.dryad.org/stash/share/HsXmnqISJFre8dF7KhW5ZxKMU7EdvuMtkEgdxM24VDs](https://data.dryad.org/stash/share/HsXmnqISJFre8dF7KhW5ZxKMU7EdvuMtkEgdxM24VDs) via

Short running title: Dynamic infectiousness impacts transmission

Key words: disease ecology; host heterogeneity; parasite transmission; susceptibility; infectiousness; epidemiological model.

Article type: Letter.

Word counts: Abstract (150 words), Main text (4,429 words)

No. references: 51.

No. tables, figures: 1 table, 4 figures.

Correspondence to: Jacob Cohen. University of Liverpool, Biosciences Building, Crown Street, Liverpool L69 7ZB. +44 151 7954528. jacob.cohen@liverpool.ac.uk.

Abstract

It is well established that heterogeneities in host susceptibility and infectiousness affect transmission, and are typically assumed to be pre-determined traits. However, they may arise dynamically during the transmission process. Specifically, while infectiousness may be an inherent trait of the recipient ('recipient-dependent'), it may instead be determined by the donor host that infected them ('donor-dependent'). We investigated how the effects of heterogeneities on transmission are affected by these contrasting scenarios by analysing two 'Susceptible-Infected' models for three metrics: the basic reproduction number (R_0), changes in heterogeneity, and equilibrium host abundance. We show that the primary driver of R_0 differs between the two scenarios: covariance between susceptibility and infectiousness for recipient-dependent, versus maximum infectiousness for donor-dependent. Consequences for equilibrium host abundance also differed, but changes in heterogeneity did not. Our results show that these scenarios change epidemiological dynamics and should be considered when exploring the consequences of host heterogeneity on transmission.

Introduction

Individuals can vary substantially in their propensity to be infected by, and to transmit, parasites (VanderWaal & Ezenwa 2016). This individual-level host heterogeneity can have significant effects on the transmission of parasites, and so affect the dynamics of transmission and patterns of infection in host populations (Woolhouse *et al.* 1997; Lloyd-Smith *et al.* 2005). One example of this is superspreaders – hosts that are disproportionately responsible for transmission of an infection in a population (Lemieux *et al.* 2021). Transmission heterogeneities can arise through variation in one or more epidemiologically-relevant host traits. Specifically, parasite transmission is a function of host susceptibility (the host's propensity to become infected following parasite exposure), host infectiousness (the capacity of an infected host to transmit parasites), and host contact rate (the rate of transmission-relevant contacts, dependent on the transmission mode of the parasite in question) (McCallum *et al.* 2017).

Among-host variation in these traits can alter parasite transmission dynamics in a host population (Dwyer *et al.* 1997; Barlow 2000; Matthews *et al.* 2006; Streicker *et al.* 2013; Stephenson *et al.* 2017). For example, modelling has shown that heterogeneity in susceptibility can reduce parasite transmission (Coutinho *et al.* 1999), heterogeneity in host infectiousness can increase variability in the probability that an epidemic will occur (White *et al.* 2018), and heterogeneity in contact rate can slow transmission speeds and reduce overall epidemic severity (Kong *et al.* 2016). Importantly, heterogeneities in these host traits can exist simultaneously, and potentially covary, raising the question of how these so-called 'coupled heterogeneities' (Vazquez-Prokopec *et al.* 2016) affect parasite transmission. Previous modelling has shown both that multiple host heterogeneities can affect transmission dynamics, as can interactions between them (Yates *et al.* 2006; Miller 2007; Hickson & Roberts 2014). Indeed, covariation between host heterogeneities can both raise and lower the basic reproduction number, R_0 , depending on the traits involved and whether the covariation is positive or negative (Vazquez-Prokopec *et al.* 2016; Lloyd *et al.* 2020).

How individual-level epidemiologically-relevant traits are determined has been generally ignored, yet is fundamental to understanding the effect of coupled heterogeneities on parasite transmission. In particular, there has been little consideration of how a host's infectiousness is determined, and the potential consequences of different determinants of infectiousness. Considering transmission from an infected donor host to a susceptible recipient host, there are two main scenarios by which the subsequent infectiousness of the newly-infected recipient host is determined. First, 'recipient-dependent' (RD), where the recipient host's infectiousness is a fixed, pre-determined characteristic of that individual, as might occur when host genotype determines infectiousness. Second, 'donor-dependent' (DD), where the recipient host's subsequent infectiousness is determined by the donor host that infected them; for example, if the parasite load received from the donor host determines the recipient host's subsequent infectiousness, such that highly infectious hosts tend to generate other highly infectious hosts (Beldomenico 2020; Wanelik *et al.* 2023). These different scenarios are likely to lead to different patterns of host infectiousness in a population, and so affect transmission, but most modelling studies of the impacts of host heterogeneity do not explicitly consider what determines host infectiousness. The majority implicitly assume RD, for example by pre-assigning susceptibility and infectiousness values to individuals (e.g., Coutinho *et al.* (1999); Yates *et al.* (2006); Miller (2007); Lloyd *et al.* (2020)), although occasionally DD-like scenarios have been used (Wanelik *et al.* 2023).

How the determination of host infectiousness mediates the effects of host heterogeneities on population-level parasite transmission has not been tested. We explore this by focusing on heterogeneities in host susceptibility and infectiousness. These two traits are likely to be determined by similar physiological and immunological mechanisms, and thus likely to be more closely linked with each other than with host contact rate (Stewart Merrill *et al.* 2021). We develop two Susceptible-Infected (SI) compartmental models that incorporate heterogeneity in susceptibility and infectiousness, one with the RD scenario, the other with the DD scenario. We analyse these models to determine how the different ways in which infectiousness is determined affect the relationship

86 between host heterogeneities in susceptibility and infectiousness, population-level parasite
87 transmission, and effects on host population dynamics. We show that how infectiousness is
88 determined can have substantial effects on parasite transmission, particularly in the driver of the
89 driver of the basic reproduction number (R_0).

Material and methods

Model Framework

The standard density-dependent SI model in a homogeneous population of size N divided into susceptible (S) and infected (I) sub-populations (Anderson & May 1991) is given by

$$\frac{dS}{dt} = bN - \beta SI - dS, \quad (1)$$

$$\frac{dI}{dt} = \beta SI - (d + \alpha)I, \quad (2)$$

where $N = S + I$, b is the birth rate, d the baseline mortality rate, and α the parasite-induced mortality rate. The transmission coefficient β , while often written as a simple constant, actually incorporates both contact rate (κ) and infection probability given a contact (ν) (Begon *et al.* 2002), yielding

$$\beta = \kappa\nu. \quad (3)$$

The infection probability ν can be further partitioned into the product of recipient susceptibility (σ) and donor infectiousness (ι),

$$\nu = \sigma\iota, \quad (4)$$

where σ and ι take values in $[0,1]$, with higher values representing greater susceptibility or greater infectiousness, respectively. Thus, host heterogeneity in susceptibility and infectiousness can be incorporated by dividing the population into sub-populations comprising individuals that share the same values of susceptibility and infectiousness. Precisely how this is done depends on whether infectiousness is determined by a RD or DD scenario.

Recipient-dependent (RD)

Under this scenario recipient hosts are assigned to an infected sub-population based on a fixed, pre-determined trait inherent to that individual. Supposing that there are n unique pairs of trait values (σ_j, ι_j) , $1 \leq j \leq n$, we divide the population into n susceptible sub-populations S_j , and n infected sub-populations I_j , where the j th sub-populations share the j th trait pair. Thus, a RD heterogeneous analogue of Equations (1)-(2) is

$$\frac{dS_j}{dt} = \frac{bN}{n} - \kappa \sigma_j S_j \sum_{m=1}^n \iota_m I_m - dS_j, \quad (5)$$

$$\frac{dI_j}{dt} = \kappa \sigma_j S_j \sum_{m=1}^n \iota_m I_m - (d + \alpha) I_j, \quad (6)$$

where we have additionally assumed that birth rate b , baseline mortality rate d , and parasite-induced mortality rate α , are equal across sub-populations. For the sake of simplicity, births are evenly distributed across susceptible sub-populations, effectively assuming non-inherited host heterogeneity, a phenomenon that has been previously observed, for example in *Daphnia magna* (Ben-Ami *et al.* 2008). We emphasise that in the RD scenario, the fixed traits of individuals determine the susceptible and infected sub-population to which they belong, so that all individuals in a susceptible sub-population move to the same infected sub-population upon becoming infected.

Donor-dependent (DD)

In this scenario, recipient hosts acquire their infectiousness trait when they become infected. Like in the RD scenario, we divide the susceptible sub-population into n_S sub-populations S_j , each with susceptibility σ_j , $1 \leq j \leq n_S$. Under the DD scenario, however, individuals are assigned the infectiousness of the donor host that infected them. We therefore define $I_{j,k}$ to be those individuals

with susceptibility σ_j that were infected by an individual with infectiousness ι_k , $0 \leq k \leq n_I$, and so now share that same infectiousness value. Thus a DD heterogeneous analogue of Equations (1)-(2) is

$$\frac{dS_j}{dt} = \frac{bN}{n_S} - \kappa \sigma_j S_j \sum_{m=1}^{n_I} \sum_{l=1}^{n_S} \iota_m I_{l,m} - dS_j, \quad (7)$$

$$\frac{dI_{j,k}}{dt} = \kappa \sigma_j \iota_k S_j \sum_{l=1}^{n_S} I_{l,k} - (d + \alpha) I_{j,k}. \quad (8)$$

b , d and α are again assumed to be equal for all infected sub-populations. Unlike the RD model, the infected sub-population that the recipient host will join is not pre-determined before infection, so individuals in the same susceptible sub-population do not always move to the same infected sub-population upon infection. As such, the DD model has n_S susceptible sub-populations and $n_S n_I$ infectious sub-populations, whereas the RD model has equal numbers of both susceptible and infected sub-populations.

Equations (7)-(8), which will be useful when quantifying population-level heterogeneity, can be simplified by defining $I_k = \sum_{j=1}^{n_S} I_{j,k}$, i.e., the sum of all individuals with the same infectiousness value, regardless of their initial susceptibility value. Summing Equation (8) over $0 \leq j \leq n_S$ yields

$$\frac{dS_j}{dt} = \frac{bN}{n_S} - \kappa \sigma_j S_j \sum_{m=1}^{n_I} \iota_m I_m - dS_j, \quad (9)$$

$$\frac{dI_k}{dt} = \kappa \iota_k I_k \sum_{m=1}^{n_S} \sigma_m S_m - (d + \alpha) I_k, \quad (10)$$

describing the dynamics of all infected individuals with infectiousness ι_k . This form of the system is useful if the prior susceptibility of infected individuals is unimportant, for example when calculating R_0 . Note that we have used the same notation in the RD and the DD models to define similar but not precisely equivalent variables, and therefore we rely on context to provide clarity about which is being referred to throughout the remainder of this work.

Quantifying population-level heterogeneity

We quantified population-level heterogeneity (hereafter referred to simply as ‘heterogeneity’) after (Laliberté & Legendre 2010), which is applicable to a wide range of systems and can deal with multiple traits and missing values (Olusoji *et al.* 2023). We undertook heterogeneity calculations in the context of two-dimensional σ, ι trait space, in which susceptibility (σ) and infectiousness (ι) form the two axes.

We first calculated the abundance-weighted centroid (c , hereafter referred to as the ‘centroid’) of the population, given simply as the population mean of each trait ($\bar{\sigma}$ and $\bar{\iota}$, Figure 1A & C). We then calculated the heterogeneity score, h , by finding the mean abundance-weighted, Euclidean distance to the centroid (e.g. z_1 in Figure 1B, z_{11} in Figure 1D) of all sub-populations. We calculated initial heterogeneity using the initial abundances of the sub-populations and final (equilibrium) heterogeneity using equilibrium sub-population abundances.

The calculation of heterogeneity differs between the RD and DD scenarios in how sub-populations were grouped, and abundances calculated. Specifically, for RD, all individuals in the same susceptible sub-population move to the same infected sub-population, and so we summed the abundances of the corresponding susceptible and infected sub-populations. These grouped sub-populations were then used to calculate h . For DD, each infected sub-population’s Euclidean distance to the centroid was calculated using both its σ and ι values (e.g. I_{11} in Figure 1D) while, because susceptible sub-populations only had a σ value, their distance to the centroid was calculated in a single dimension (e.g. S_1 in Figure 1D), and so there were no grouped sub-populations used in calculating h . The formulae for heterogeneity calculations for both the RD and DD scenarios can be found in the Supplementary Information (SI).

Model Analyses

We analysed both the RD and DD scenarios under three heterogeneity contexts:

1) *Bipartite heterogeneity*

Where the population is divided into sub-populations corresponding to two distinct pairs of susceptibility and infectiousness values.

2) *Tripartite isometric heterogeneity*

Where the population is divided into sub-populations corresponding to three distinct pairs of susceptibility and infectiousness values, equidistant from each other in σ, ι trait space.

3) *Tripartite non-isometric heterogeneity*

Where the population is divided into sub-populations corresponding to three distinct pairs of susceptibility and infectiousness values, but which are not necessarily equidistant in σ, ι trait space.

Here we present analyses relating to context 1; contexts 2 and 3 are presented in the SI.

For all quantitative analyses we set the initial number of susceptible sub-populations to 49 and the number of infected sub-populations to $\frac{1}{n}$ (RD) or $\frac{1}{n_s}$ (DD). Initial mean population susceptibility and infectiousness trait values were 0.5; thus $\sigma_2 = 1 - \sigma_1$ and $\iota_2 = 1 - \iota_1$. All other parameter values were the same for all analyses (Table 1). By varying σ_1 and ι_1 , we varied the initial population heterogeneity while maintaining the same initial mean population trait values. Hence, the effects of changing heterogeneity were decoupled from the effects of changing initial mean population trait values.

We generated 2,601 unique combinations of σ and ι trait values, and used these to analyse both the RD and DD models to understand how heterogeneity in susceptibility and infectiousness affected three key descriptors of epidemiological dynamics: (i) the basic reproduction number (R_0), a measure of epidemic potential (Anderson & May 1991), (ii) the change in heterogeneity between the initial and final state of the system, indicating how heterogeneity changes with epidemic progression; and (iii) the equilibrium host population abundance, which quantifies the impact of the parasite on the host population.

201

202 **Calculating R_0**

203 R_0 predicts the risk of an epidemic occurring, as well as the size and severity of that epidemic
204 (Anderson & May 1991; Heffernan *et al.* 2005), and also the effort needed to control and eliminate a
205 parasite from a population (Roberts 2007). Thus, understanding the effect of heterogeneity on R_0
206 provides considerable insight into how host heterogeneity in susceptibility and infectiousness affects
207 parasite transmission through a population.

208 We calculated R_0 using next generation matrices (Diekmann *et al.* 2010) (shown in full in the SI) for
209 the two different scenarios, as:

210 **RD:**

$$211 \quad R_0 = \frac{\kappa}{d + \alpha} \sum_{j=1}^n \sigma_j \iota_j S_j, \quad (11)$$

212 **DD:**

$$213 \quad R_0 = \frac{\kappa \iota_{\max}}{d + \alpha} \sum_{j=1}^{n_s} \sigma_j S_j, \quad (12)$$

214 where ι_{\max} is the maximum infectiousness value across all sub-populations.

215

216 **Equilibrium Analyses**

217 When possible we calculated the equilibrium solutions of Equations (5)-(8) analytically. For parameter
218 values for which this was not possible, we solved the system numerically over 50,000 time steps, which
219 was sufficiently long to reach equilibrium. Any sub-population with susceptibility $\sigma = 0$ (*i.e.*,
220 completely resistant to infection) experiences unbounded growth, and so such cases were omitted
221 from equilibrium analyses.

222 We also used these equilibrium solutions to calculate equilibrium population-level heterogeneity
223 (following the method described above) to test whether the population-level heterogeneity changed
224 with epidemiological progress.

225

226 **Software packages**

227 Plots were generated in R (R Core Team 2022) using packages ggplot2 (Wickham 2016), ggforce
228 (Pedersen 2022a), scales (Wickham & Seidel 2022), showtext (Qiu 2022), pBrackets (Schulz 2021),
229 patchwork (Pedersen 2022b) and latex2exp (Meschiari 2022). Equilibrium analyses were conducted
230 using Mathematica (Wolfram Research Inc. 2022). Heterogeneity and R_0 values were calculated in R
231 (R Core Team 2022).

Results

Here we present the results for the analyses of the bipartite heterogeneity context. The results for the other contexts were broadly consistent with those of Scenario 1 and are described in the SI.

(i) Heterogeneity and R_0

Recipient-dependent

Depending on the population-level covariance between susceptibility and infectiousness values, R_0 may increase (Figure 2A, red points), decrease (Figure 2A, blue points) or remain the same as the homogenous case (Figure 2A, yellow points) as heterogeneity increases. Mapping R_0 values onto σ, ι trait space (Figure 2B), where the two subpopulations are mirrored across the centre point ($\sigma_2 = 1 - \sigma_1$ and $\iota_2 = 1 - \iota_1$), shows that R_0 remains unchanged from the homogeneous state ($h = 0$), even at high levels of heterogeneity, if that heterogeneity is in one trait only (Figure 2B yellow shading).

When there is positive covariation between susceptibility and infectiousness, R_0 increases relative to the homogenous state (Figure 2B, Supplementary Equation (S13)). The largest R_0 value occurs when one sub-population has maximal infectiousness and susceptibility values of 1, while the other sub-population has values of 0 for both; *i.e.*, the sub-populations lie at extremes of the positive diagonal in σ, ι trait space (Figure 2B). Conversely, when there is negative covariation between susceptibility and infectiousness R_0 is reduced relative to the homogenous case (Figure 2B). In the extreme case, when one sub-population has an infectiousness value of 1 and a susceptibility value of 0 (completely resistant hosts), and the other sub-population has a susceptibility of 1 and infectiousness of 0 (completely dead-end hosts), such that they lie at extremes of the negative diagonal in σ, ι trait space, no individuals can both be infected and transmit onwards, resulting in an R_0 value of 0 (Figure 2B).

The bifurcating distribution of points that occurs at high heterogeneity (Figure 2A) is due to the boundaries of σ, ι trait space that necessarily restrict the number of possible trait combinations (*i.e.*,

where both susceptibility and infectiousness values lie between 0 and 1 for all sub-populations) at higher levels of heterogeneity. At maximum heterogeneity there are only two possible configurations of the two sub-populations in σ, ι trait space, lying at the opposite extremes of the diagonals in σ, ι trait space, resulting in just two points (Figure 2A).

In summary, increasing heterogeneity in the RD scenario can lead to increasingly divergent R_0 values compared to the homogeneous simulation, where the direction of this divergence (positive or negative) is determined by the population-level covariance between susceptibility and infectiousness. When that covariance equals zero (heterogeneity in either susceptibility or infectiousness, but not both) then R_0 is unchanged even as heterogeneity increases.

Donor-dependent

The DD scenario produces different results from the RD scenario. The overall pattern is that increasing heterogeneity does not reduce R_0 relative to the homogenous case (Figure 2C), and more generally that heterogeneity does not influence R_0 . In particular, changes in susceptibility alone do not affect R_0 , whereas changes in infectiousness do (Figure 2D).

The driver of R_0 is the maximum infectiousness value in the population (Figure 2C, Supplementary Equation (S13)). R_0 is independent of susceptibility because, assuming equal susceptible sub-population sizes, it has a fixed mean value across the population (details in SI). R_0 changes only along the infectiousness axis (Figure 2D), but not along the susceptibility axis. This means that while heterogeneity can be increased by changing susceptibility trait values, R_0 will stay the same as in the homogenous case in the absence of changes in infectiousness. Equally, for the same overall degree of heterogeneity (*i.e.*, vertical slice in Figure 2C) an increase in heterogeneity in infectiousness (and

therefore a necessary decrease in heterogeneity in susceptibility) increases R_0 . Susceptibility can only affect R_0 when the initial susceptible sub-population abundances are not equal (see SI).

Model comparison

In summary, both the RD and DD scenarios show that increasing heterogeneity can lead to increasingly divergent R_0 values compared to the homogeneous case, but that the driver of those R_0 values differs between the two scenarios. In the RD scenario, R_0 is driven by covariation between susceptibility and infectiousness; in the DD scenario R_0 is driven by the maximum infectiousness in the population.

(ii) Change in heterogeneity

To understand how epidemic progress affects population-level heterogeneity we compared initial heterogeneity and its value at equilibrium. For both the RD and DD scenarios there is generally very little change in population-level heterogeneity throughout the epidemic (Figure 3).

(iii) Host abundance

Equilibrium total host abundance generally increases with increasing initial heterogeneity, as does the variability in equilibrium abundance, in both the RD and DD scenarios (Figure 4). However, the specific aspects of these relationships differ between the two scenarios.

Recipient-dependent

Here there is a complex relationship between initial heterogeneity and host equilibrium abundance (Figure 4A). Equilibrium abundances are grouped into parabolic ‘clusters’ where each cluster has

increasing and decreasing equilibrium abundances that diverge from a baseline abundance as heterogeneity increases. These clusters are determined by the minimum susceptibility value in the simulation; each simulation in a cluster has the same population-level minimum susceptibility value (and therefore also the same maximum susceptibility value). Clusters are ordered based on these minimum susceptibility values; those with the lowest minimum susceptibility values have the highest abundances. This is because in populations with low minimum susceptibility values fewer individuals become infected, so that fewer hosts are exposed to parasite-induced mortality (α), thus increasing overall host abundance.

The within-cluster divergence seen with increasing heterogeneity is because of increasingly divergent infectiousness values in the population. In σ, ι trait space, all the simulations within a cluster have the same pair of σ values for the two sub-populations in the population, so that an increase in heterogeneity is achieved by divergence in the two infectiousness values. This divergence, and thus increase in heterogeneity, leads to changes in R_0 within a cluster that subsequently impacts equilibrium host abundance; high R_0 values lead to lower abundances (the lower red tail of a cluster in Figure 4A), while low R_0 values lead to higher abundances (the upper blue tail of a cluster in Figure 4A).

Donor-dependent

In this scenario there are also clusters determined by the minimum susceptibility value within a simulation, but these clusters are near-vertical lines, suggesting that heterogeneity has little effect on equilibrium host abundance (Figure 4B). Consistent with the RD scenario, within-cluster host equilibrium abundance is maximised when R_0 is minimised, which occurs at the lowest maximum population-level infectiousness value. Increasing maximum infectiousness for a given cluster increases R_0 , and so reduces equilibrium host abundance. The DD scenario generally shows a lower maximum

324 equilibrium host abundance than the RD scenario because the minimum R_0 values for the RD scenario
325 are lower than the DD scenario.

Discussion

Our results show that the process by which host infectiousness is determined, specifically whether it is RD or DD, affects the relationships between host heterogeneity in susceptibility and infectiousness and epidemiological outcomes. While existing theory shows that host heterogeneity in susceptibility and infectiousness can affect population-level parasite transmission (e.g. Lloyd *et al.* (2020)), our findings clarify that these effects differ considerably between RD and DD scenarios.

We find that while R_0 changes with increasing heterogeneity in both scenarios, there is a notable contrast between the two scenarios in both the drivers and direction of those changes. The RD scenario shows divergent R_0 values as heterogeneity increases, determined by the covariance between susceptibility and infectiousness. This finding is supported by previous modelling: three models of vector-borne infections, where infectiousness was an inherent host trait, *i.e.* RD, incorporated host heterogeneity in susceptibility and infectiousness and found that positive covariance between heterogeneities led to an increase in R_0 relative to the homogeneous case, while negative covariance led to a decrease (Dietz 1980; Koella 1991; Vazquez-Prokopec *et al.* 2016). Thus, they showed that in a RD scenario population-level covariance between susceptibility and infectiousness determines R_0 , consistent with our findings.

In contrast, we find that the DD scenario results in R_0 values that are determined by the maximum infectiousness in a population, such that R_0 increases as heterogeneity in infectiousness increases. Heterogeneity in susceptibility is largely irrelevant for the DD scenario, only becoming relevant if abundances are markedly different between sub-populations. Though there are fewer other studies that consider DD-like scenarios, one example is the hypothesis that the SARS-CoV-2 transmission pattern may be due to superspreaders tending to generate new superspreaders, for example through a dose-dependent effect (Beldomenico 2020). A model exploring how R_0 responded to the scenario described in Beldomenico (2020) compared to the null model in which superspreaders appeared randomly, showed that R_0 increases with an increase in the probability that a superspreader generates

additional superspreaders (Wanelik *et al.* 2023). Thus, moving from the null model to a DD-like scenario increased R_0 , suggesting that the DD scenario tends to increase R_0 , which aligns with our findings.

Counterintuitively, we did not find a noticeable divergence between the RD and DD scenarios in how population-level heterogeneity changed during an epidemic. In the DD scenario we expected to see a loss of heterogeneity over time because the infected sub-population with the highest infectiousness value in the population becomes dominant as the epidemic progresses, ultimately excluding less infectious donors. However, heterogeneity is calculated by taking the mean abundance-weighted distance of the sub-populations to the centroid. Thus, despite the DD scenario losing infected sub-populations at equilibrium (and leading to maximally infectious hosts over time), the weighting of the heterogeneity score with the generally larger susceptible sub-populations ensures that there is no considerable loss in heterogeneity at equilibrium.

In contrast, the consequences of heterogeneity for equilibrium total host abundances are different between the two scenarios. While in both the RD and DD scenarios host abundance tends to increase with increasing heterogeneity, heterogeneity has less influence on the equilibrium host abundance in the DD scenario, compared to the RD scenario. Furthermore, for a given susceptibility value (*i.e.*, within a cluster) the infectiousness scenario determines whether there are divergent (RD) or monotonic (DD) changes in equilibrium host abundance, a pattern that becomes more pronounced at higher levels of heterogeneity.

Empirical examples matching assumptions of the RD scenario include the finding that canaries' nutritional status can affect their subsequent infectiousness with avian malaria (Cornet *et al.* 2014), rabbit myxoma virus infection status determines its infectiousness for co-infecting nematodes (Cattadori *et al.* 2007), as well as several examples of different host strains exhibiting varying levels of infectiousness when infected with the same parasite isolates (Bolas-Fernandez & Wakelin 1989; Jørgensen *et al.* 1998; Dorfman *et al.* 2024). Genetic variance in host infectiousness was then

definitively demonstrated in *Scophthalmus maximus* (Turbot) infected with a ciliate parasite (Anacleto *et al.* 2019). An example of the DD scenario comes from calves that were infected with three different doses of bovine viral diarrhoea virus (BVDV) where the most infectious were those given the highest viral dose, due to a longer infectious period (Strong *et al.* 2015). Similar patterns have been found with a number of other host-parasite systems (Gaskell & Povey 1979; Mumford *et al.* 1990; Zarkov 2012).

In reality, host-parasite systems are unlikely to be fully described by either the RD or DD scenarios, instead likely falling somewhere between the two. For instance, though the calves challenged with the highest dose of BVDV had a higher infectiousness than other treatments, there was still within-dose group heterogeneity in infectiousness (Strong *et al.* 2015). This within-group heterogeneity may have been caused by traits inherent to the individual calves, suggesting that while this host-parasite system might be best described by DD infectiousness there are still aspects of RD infectiousness at play. The reverse can also be true. For example, although myxoma-infected rabbits may be more nematode infectious (Cattadori *et al.* 2007), aligning with RD infectiousness, there may still be some DD infectiousness involved. Specifically, the nematode spreads to other hosts when its eggs are released into the environment in a rabbit's faeces, hatch into larvae and are then eaten by another rabbit (Cattadori *et al.* 2007). So, there is a chance that a rabbit will become more infectious when it is infected by a rabbit with a high infectiousness, because a highly infectious rabbit is likely to leave many nematode eggs to hatch in a patch of the environment, potentially leading to many of those larvae infecting the same host at the same time. If that is the case, then the susceptible rabbit would become highly infectious in turn. Therefore, in most cases R_0 will be affected by both the covariance between susceptibility and infectiousness as well as the maximum infectiousness in the population, though which of these two measures is more influential will depend on where on the spectrum of RD to DD that specific host-parasite system exists.

Previous work has typically treated the infectiousness determination process as a black box, generally assuming it is a fixed, pre-determined property of the recipient host, overlooking its potential

importance in influencing the effects of host heterogeneity on parasite transmission. Yet this process can have real-world consequences. For instance, there is interest in breeding parasite resistant livestock to reduce the substantial economic and climatic costs caused by parasites in livestock systems (Knap & Doeschl-Wilson 2020). However, it will be important to consider how infectiousness is determined in the specific host-parasite system of interest, as it might be necessary to select for different traits in the livestock depending on where the host-parasite system falls along the infectiousness determination spectrum. For example, breeding for reduced parasite susceptibility in a RD scenario (*i.e.*, resistance), versus focusing on reducing parasite shedding in a DD scenario. We have demonstrated the importance of explicitly considering the way in which infectiousness is determined, showing that ignoring it could lead to an incomplete understanding of the effects of host heterogeneities on parasite transmission. A failure to do so could have consequences for both future theoretical and empirical work.

Acknowledgements

JAC was funded by a PhD studentship from the 'Adapting to the Challenges of a Changing Environment (ACCE)' Doctoral Training Partnership funded by the Natural Environment Research Council (NERC) (Grant NE/S00713X/1). ADD was funded by a NERC Pushing the Frontiers grant (Grant NE/X01424X/1).

References

- Anacleto, O., Cabaleiro, S., Villanueva, B., Saura, M., Houston, R.D., Woolliams, J.A. *et al.* (2019). Genetic differences in host infectivity affect disease spread and survival in epidemics. *Scientific Reports*, 9, 4924.
- Anderson, R.M. & May, R.M. (1991). *Infectious Diseases of Humans*. Oxford University Press.
- Barlow, N.D. (2000). Non-linear transmission and simple models for bovine tuberculosis. *Journal of Animal Ecology*, 69, 703-713.
- Begon, M., Bennett, M., Bowers, R.G., French, N.P., Hazel, S. & Turner, J. (2002). A clarification of transmission terms in host-microparasite models: numbers, densities and areas. *Epidemiology & Infection*, 129, 147-153.
- Beldomenico, P.M. (2020). Do superspreaders generate new superspreaders? A hypothesis to explain the propagation pattern of COVID-19. *International Journal of Infectious Diseases*, 96, 461-463.
- Ben-Ami, F., Regoes, R.R. & Ebert, D. (2008). A quantitative test of the relationship between parasite dose and infection probability across different host–parasite combinations. *Proceedings of the Royal Society B: Biological Sciences*, 275, 853-859.
- Bolas-Fernandez, F. & Wakelin, D. (1989). Infectivity of *Trichinella* isolates in mice is determined by host immune responsiveness. *Parasitology*, 99, 83-88.
- Cattadori, I.M., Albert, R. & Boag, B. (2007). Variation in host susceptibility and infectiousness generated by co-infection: the myxoma–*Trichostrongylus retortaeformis* case in wild rabbits. *Journal of the Royal Society Interface*, 4, 831-840.
- Cornet, S., Bichet, C., Larcombe, S., Faivre, B. & Sorci, G. (2014). Impact of host nutritional status on infection dynamics and parasite virulence in a bird-malaria system. *Journal of Animal Ecology*, 83, 256-265.

Coutinho, F.A.B., Massad, E., Lopez, L.F., Burattini, M.N., Struchiner, C.J. & Azevedo-Neto, R.S.d.
 (1999). Modelling heterogeneities in individual frailties in epidemic models. *Mathematical and
 Computer Modelling*, 30, 97-115.

Diekmann, O., Heesterbeek, J. & Roberts, M.G. (2010). The construction of next-generation matrices
 for compartmental epidemic models. *Journal of the Royal Society Interface*, 7, 873-885.

Dietz, K. (1980). Models for vector-borne parasitic diseases. In: *Vito Volterra Symposium on
 Mathematical Models in Biology*. Springer, pp. 264-277.

Dorfman, B., Marcos-Hadad, E., Tadmor-Levi, R. & David, L. (2024). Disease resistance and infectivity
 of virus susceptible and resistant common carp strains. *Scientific Reports*, 14, 4677.

Dwyer, G., Elkinton, J.S. & Buonaccorsi, J.P. (1997). Host heterogeneity in susceptibility and disease
 dynamics: tests of a mathematical model. *The American Naturalist*, 150, 685-707.

Gaskell, R. & Povey, R. (1979). The dose response of cats to experimental infection with feline viral
 rhinotracheitis virus. *Journal of Comparative Pathology*, 89, 179-191.

Heffernan, J.M., Smith, R.J. & Wahl, L.M. (2005). Perspectives on the basic reproductive ratio.
Journal of the Royal Society Interface, 2, 281-293.

Hickson, R. & Roberts, M. (2014). How population heterogeneity in susceptibility and infectivity
 influences epidemic dynamics. *Journal of Theoretical Biology*, 350, 70-80.

Jørgensen, L., Leathwick, D., Charleston, W., Godfrey, P., Vlassoff, A. & Sutherland, I. (1998).
 Variation between hosts in the developmental success of the free-living stages of trichostrongyle
 infections of sheep. *International Journal for Parasitology*, 28, 1347-1352.

Knap, P.W. & Doeschl-Wilson, A. (2020). Why breed disease-resilient livestock, and how? *Genetics
 Selection Evolution*, 52, 1-18.

Koella, J.C. (1991). On the use of mathematical models of malaria transmission. *Acta Tropica*, 49, 1-
 25.

466 Kong, L., Wang, J., Han, W. & Cao, Z. (2016). Modeling heterogeneity in direct infectious disease
467 transmission in a compartmental model. *International Journal of Environmental Research and Public*
468 *Health*, 13, 253.

469 Laliberté, E. & Legendre, P. (2010). A distance-based framework for measuring functional diversity
470 from multiple traits. *Ecology*, 91, 299-305.

471 Lemieux, J.E., Siddle, K.J., Shaw, B.M., Loreth, C., Schaffner, S.F., Gladden-Young, A. *et al.* (2021).
472 Phylogenetic analysis of SARS-CoV-2 in Boston highlights the impact of superspreading events.
473 *Science*, 371, eabe3261.

474 Lloyd-Smith, J.O., Schreiber, S.J., Kopp, P.E. & Getz, W.M. (2005). Superspreading and the effect of
475 individual variation on disease emergence. *Nature*, 438, 355-359.

476 Lloyd, A.L., Kitron, U., Perkins, T.A., Vazquez-Prokopec, G.M. & Waller, L.A. (2020). The basic
477 reproductive number for disease systems with multiple coupled heterogeneities. *Mathematical*
478 *Biosciences*, 321, 108294.

479 Matthews, L., McKendrick, I.J., Ternent, H., Gunn, G., Synge, B. & Woolhouse, M. (2006). Super-
480 shedding cattle and the transmission dynamics of *Escherichia coli* O157. *Epidemiology & Infection*,
481 134, 131-142.

482 McCallum, H., Fenton, A., Hudson, P.J., Lee, B., Levick, B., Norman, R. *et al.* (2017). Breaking beta:
483 deconstructing the parasite transmission function. *Philosophical Transactions of the Royal Society B:*
484 *Biological Sciences*, 372, 20160084.

485 Meschiari, S. (2022). latex2exp: Use LaTeX Expression in Plots.

486 Miller, J.C. (2007). Epidemic size and probability in populations with heterogeneous infectivity and
487 susceptibility. *Physical Review E*, 76, 010101.

488 Mumford, J.A., Hannant, D. & Jessett, D. (1990). Experimental infection of ponies with equine
489 influenza (H3N8) viruses by intranasal inoculation or exposure to aerosols. *Equine Veterinary Journal*,
490 22, 93-98.

491 Olusoji, O.D., Barabás, G., Spaak, J.W., Fontana, S., Neyens, T., De Laender, F. *et al.* (2023).
 492 Measuring individual-level trait diversity: a critical assessment of methods. *Oikos*, 2023, e09178.
 493 Pedersen, T.L. (2022a). ggforce: Accelerating 'ggplot2'.
 494 Pedersen, T.L. (2022b). patchwork: The Composer of Plots.
 495 Qiu, Y. (2022). showtext: Using Fonts More Easily in R Graphs.
 496 R Core Team (2022). R: A language and environment for statistical computing. R Foundation for
 497 Statistical Computing Vienna, Austria.
 498 Roberts, M. (2007). The pluses and minuses of R0. *Journal of the Royal Society Interface*, 4, 949-961.
 499 Schulz, A. (2021). pBrackets: Plot Brackets.
 500 Stephenson, J.F., Young, K.A., Fox, J., Jokela, J., Cable, J. & Perkins, S.E. (2017). Host heterogeneity
 501 affects both parasite transmission to and fitness on subsequent hosts. *Philosophical Transactions of*
 502 *the Royal Society B: Biological Sciences*, 372, 20160093.
 503 Stewart Merrill, T.E., Rapti, Z. & Cáceres, C.E. (2021). Host controls of within-host disease dynamics:
 504 insight from an invertebrate system. *The American Naturalist*, 198, 317-332.
 505 Streicker, D.G., Fenton, A. & Pedersen, A.B. (2013). Differential sources of host species heterogeneity
 506 influence the transmission and control of multihost parasites. *Ecology Letters*, 16, 975-984.
 507 Strong, R., La Rocca, S.A., Paton, D., Bensaude, E., Sandvik, T., Davis, L. *et al.* (2015). Viral dose and
 508 immunosuppression modulate the progression of acute BVDV-1 infection in calves: evidence of long
 509 term persistence after intra-nasal infection. *PLOS ONE*, 10, e0124689.
 510 VanderWaal, K.L. & Ezenwa, V.O. (2016). Heterogeneity in pathogen transmission: mechanisms and
 511 methodology. *Functional Ecology*, 30, 1606-1622.
 512 Vazquez-Prokopec, G.M., Perkins, T.A., Waller, L.A., Lloyd, A.L., Reiner Jr, R.C., Scott, T.W. *et al.*
 513 (2016). Coupled heterogeneities and their impact on parasite transmission and control. *Trends in*
 514 *Parasitology*, 32, 356-367.
 515 Wanelik, K.M., Begon, M., Fenton, A., Norman, R.A. & Beldomenico, P.M. (2023). Positive feedback
 516 loops exacerbate the influence of superspreaders in disease transmission. *iScience*, 26.

517 White, L.A., Forester, J.D. & Craft, M.E. (2018). Covariation between the physiological and behavioral
 518 components of pathogen transmission: host heterogeneity determines epidemic outcomes. *Oikos*,
 519 127, 538-552.

520 Wickham, H. (2016). *ggplot2: Elegant Graphics for Data Analysis*. Springer-Verlag New York.

521 Wickham, H. & Seidel, D. (2022). *scales: Scale Functions for Visualization*.

522 Wolfram Research Inc. (2022). *Mathematica*. Wolfram Research Inc. Champaign, Illinois.

523 Woolhouse, M.E., Dye, C., Etard, J.-F., Smith, T., Charlwood, J., Garnett, G. *et al.* (1997).
 524 Heterogeneities in the transmission of infectious agents: implications for the design of control
 525 programs. *Proceedings of the National Academy of Sciences*, 94, 338-342.

526 Yates, A., Antia, R. & Regoes, R.R. (2006). How do pathogen evolution and host heterogeneity
 527 interact in disease emergence? *Proceedings of the Royal Society B: Biological Sciences*, 273, 3075-
 528 3083.

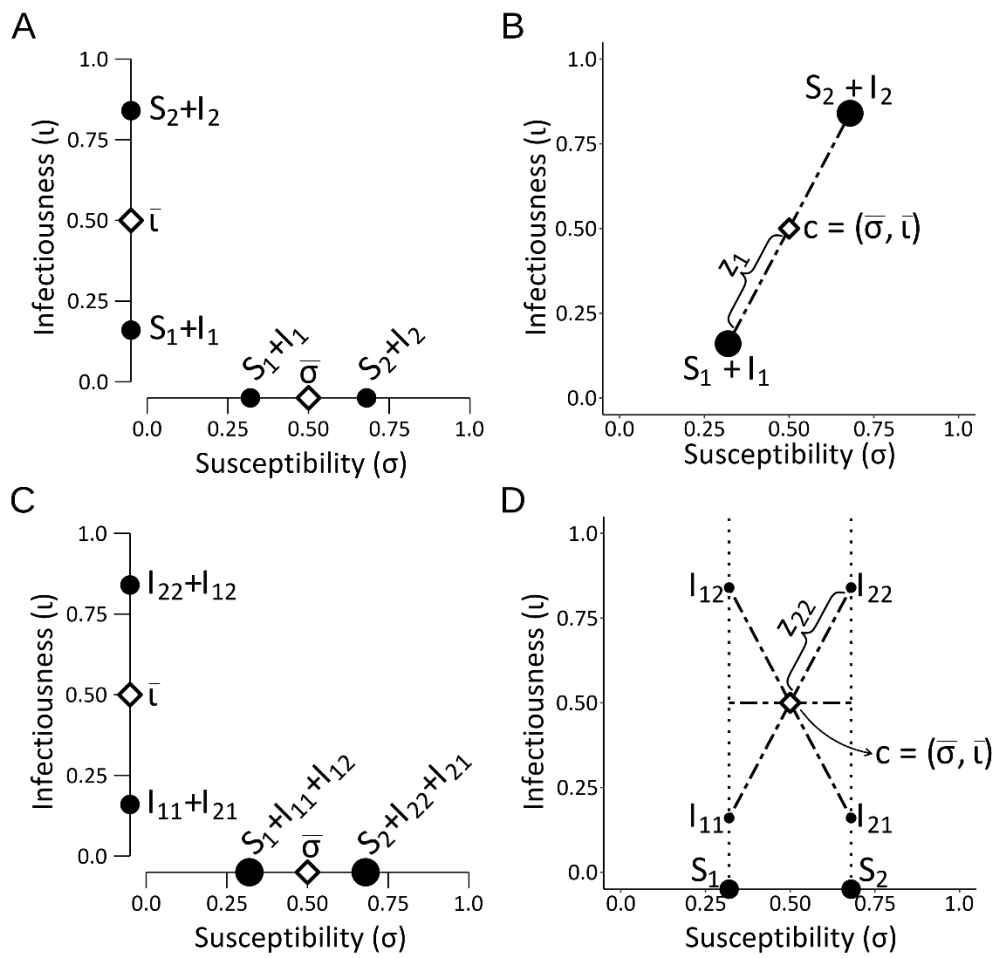
529 Zarkov, I. (2012). The importance of inoculation dose of avian H6N2 influenza a virus on virus
 530 shedding of *Anas platyrhynchos* ducks after induced generalised infection. *Trakia Journal of Sciences*,
 531 10, 58-61.

532

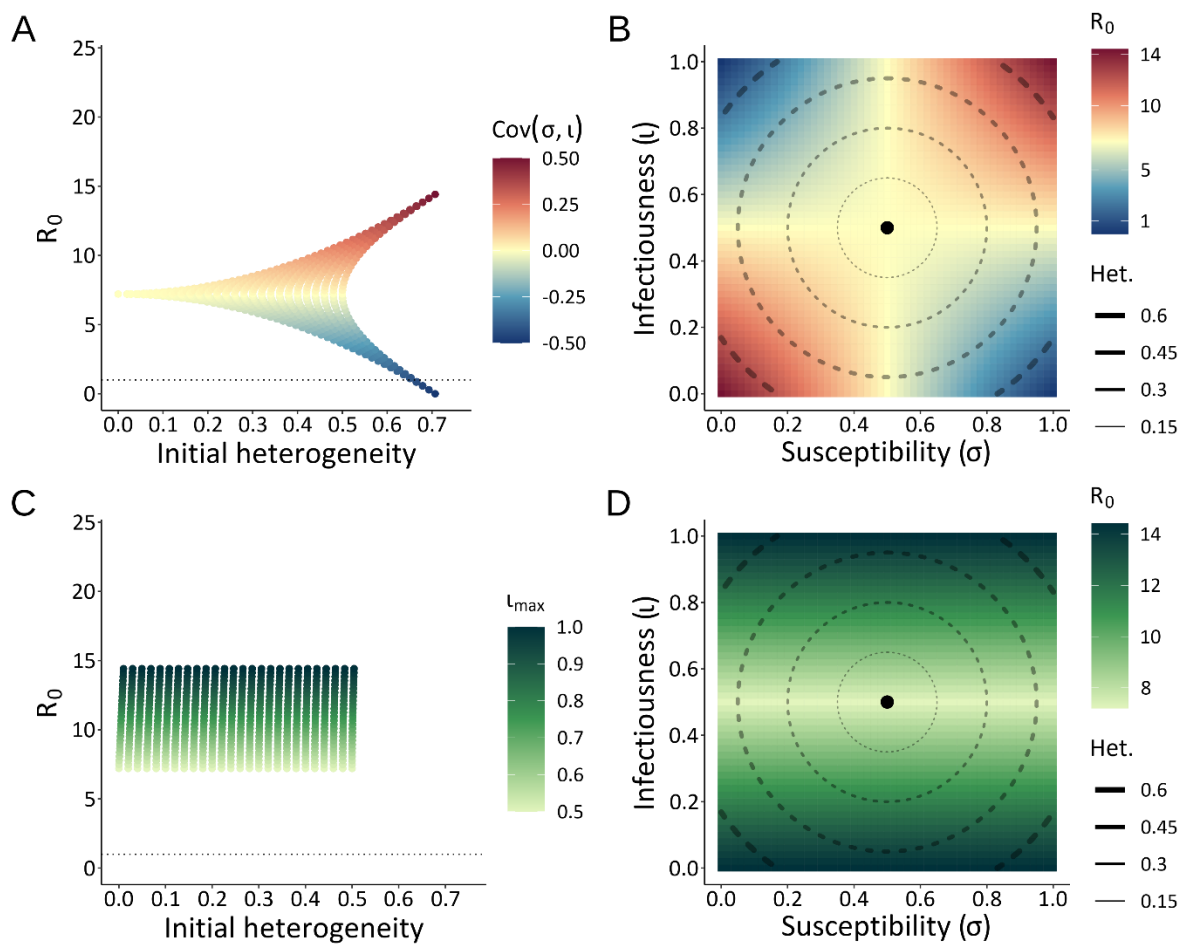
533 Table 1. Parameter definitions and values for all analyses of the RD and DD models.

Model parameter	Definition	Value
κ	Contact rate per individual per time	0.5
b	Birth rate per time	1.5
d	Mortality rate per time	1
α	Parasite-induced mortality rate per time	0.7

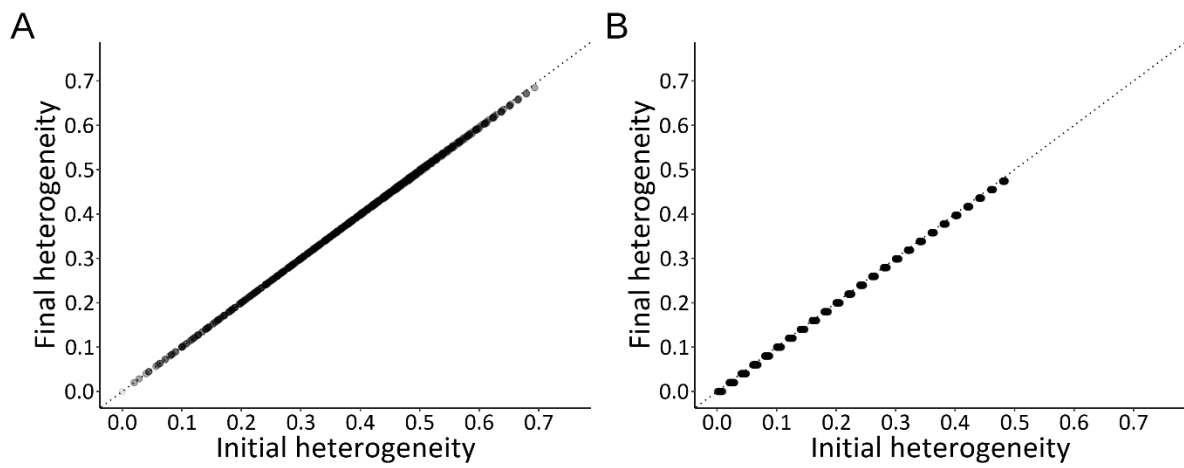
534



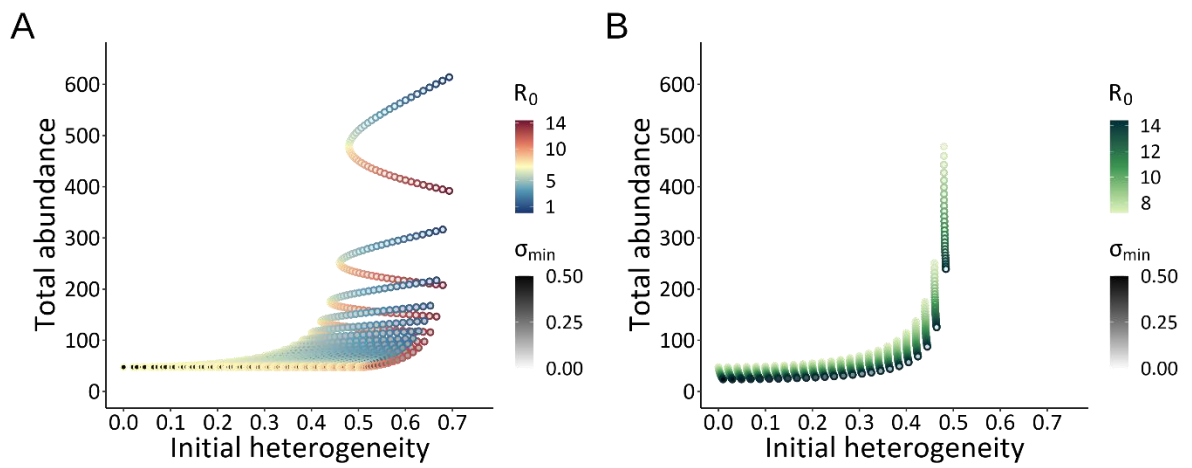
535



536



537



538

Figure 1. Schematic representation for calculating heterogeneity for the RD (A, B) and DD (C, D) scenarios. For both the RD and DD scenarios the population mean susceptibility ($\bar{\sigma}$) and population mean infectiousness ($\bar{\iota}$) are calculated in a single dimension (A and C). The sizes of the black dots indicate the relative abundances of the relevant sub-populations. (B) Heterogeneity for the RD scenario is the mean Euclidean distance (z_j), weighted by the abundance of each sub-population, to the centroid (c). (D) Heterogeneity for the DD scenario is the mean of the Euclidean distances (z_{jk}) of the infected sub-populations to the centroid, and the single dimension distance (σ) of the susceptible sub-populations, weighted by the abundance of each sub-population; here the values for S_1 and S_2 form lines rather than points in σ, ι trait space because they have no infectiousness values. In all panels the diameters of the black circles represent the abundance of the sub-population.

Figure 2. The effect of initial heterogeneity on R_0 for the RD (A, B) and DD (C, D) scenarios. The dotted line in (A, B) is where $R_0 = 1$. For RD (A) R_0 can change as initial heterogeneity increases, and with the covariance between susceptibility (σ) and infectiousness (ι), as indicated by the colour bar. (B) shows R_0 (the colour scale) plotted in σ, ι trait space with the centroid (c) at $\sigma = \iota = 0.5$, and concentric dashed-line circles showing heterogeneity; the positions of the sub-populations are mirrored across the centroid ($\sigma_2 = 1 - \sigma_1$ and $\iota_2 = 1 - \iota_1$). For DD (C) R_0 does not change as initial heterogeneity increases, but scales with maximum infectiousness (ι_{\max}), as indicated by the colour bar. (D) is the DD version of panel (B), but note that the R_0 scales differ between (B) and (D).

Figure 3. Change in heterogeneity from the initial sub-population values to their equilibrium values (the dotted line shows $y = x$ in both panels). (A) RD scenario, (B) DD scenario. Each point represents one simulation; points are light grey, such that darker points represent multiple, overlapping points.

563 Figure 4. Effect of initial heterogeneity on equilibrium total host abundance. (A) RD, (B) DD. In both
564 panels the colour bar shows the R_0 value for each simulation, corresponding to the outline of each
565 point, and the greyscale bar shows the minimum population-level susceptibility value corresponding
566 to the fill of each point.